Lentivector Transduction Improves Outcomes Over Transplantation of Human HSCs Alone in NOD/SCID/Fabry Mice

Natalia Pacienza[1], Makoto Yoshimitsu[1,2], Nobuo Mizue[1], Bryan CY Au[1], James CM Wang[1], Xin Fan[1], Toshihiro Takenaka[2] and Jeffrey A Medin[1,3,4]

[1]University Health Network, Toronto, Ontario, Canada; [2]Division of Cardiac Repair and Regeneration, Graduate School of Medical and Dental Sciences, Kagoshima University, Kagoshima, Japan; [3]Department of Medical Biophysics, University of Toronto, Toronto, Ontario, Canada; [4]Institute of Medical Sciences, University of Toronto, Toronto, Ontario, Canada

Fabry disease is a lysosomal storage disorder caused by a deficiency of α-galactosidase A (α-gal A) activity that results in progressive globotriaosylceramide (Gb_3) deposition. We created a fully congenic nonobese diabetic (NOD)/severe combined immunodeficiency (SCID)/Fabry murine line to facilitate the *in vivo* assessment of human cell-directed therapies for Fabry disease. This pure line was generated after 11 generations of backcrosses and was found, as expected, to have a reduced immune compartment and background α-gal A activity. Next, we transplanted normal human $CD34^+$ cells transduced with a control (lentiviral vector-enhanced green fluorescent protein (LV-eGFP)) or a therapeutic bicistronic LV (LV-α-gal A/internal ribosome entry site (IRES)/hCD25). While both experimental groups showed similar engraftment levels, only the therapeutic group displayed a significant increase in plasma α-gal A activity. Gb_3 quantification at 12 weeks revealed metabolic correction in the spleen, lung, and liver for both groups. Importantly, only in the therapeutically-transduced cohort was a significant Gb_3 reduction found in the heart and kidney, key target organs for the amelioration of Fabry disease in humans.

Received 13 July 2011; accepted 6 March 2012;advance online publication 3 April 2012. doi:10.1038/mt.2012.64

INTRODUCTION

Fabry disease is an X-linked lysosomal storage disorder caused by a deficiency in the hydrolase, α-galactosidase A (α-gal A), which catalyzes the cleavage of the terminal molecule of galactose from neutral glycosphingolipids. The main consequence of this metabolic anomaly is a progressive lipid accumulation throughout the body, particularly involving globotriaosylceramide (Gb_3).[1] The accumulation of Gb_3 in endothelial cells from the kidneys, heart, and brain leads to life-threatening complications and early death. Compared to the normal population, Fabry patient life expectancy is reduced 15 and 20 years for heterozygous women and hemizygous men, respectively, with a steep decline in survival after 35 years of age.[2,3] Enzyme replacement therapy (ERT) has now been commercially available as specific treatment for Fabry disease for almost 10 years. During this period, several clinical trials have shown some positive effects from ERT in treating pain, reducing heart size, stabilizing kidney function, and improving hearing and sweating.[4,5] However, this therapy is hampered by both economic (~250,000 USD/patient/year) and therapeutic (variable clinical efficacy) considerations.[6,7] Furthermore, it has been demonstrated that ERT is effective for stabilizing renal function and reducing left ventricular wall thickness, two of the major clinical concerns on Fabry disease, only when it is provided at an early phase of the disease.[8–11] Moreover, ERT constitutes only a short-term treatment, given the limited half-life of the enzyme product *in vivo*, and does not solve the underlying genetic defect of this disorder.

Fabry disease is a natural candidate for gene therapy. α-Gal A can diffuse from engineered cells and be subsequently taken up by bystander deficient cells through mannose 6-phosphate receptor–mediated salvage pathway in a process called metabolic cooperativity.[12,13] Previously, we demonstrated that by using genetically modified murine bone marrow cells it is possible to attain long-term enzymatic correction and Gb_3 reduction in primary and secondary transplanted Fabry mice.[14] By using different integrating viral vectors we were able to significantly increase the α-gal A activity of mobilized Fabry patient hematopoietic stem cells (HSCs).[15,16] Here, we aimed to generate a more suitable Fabry mouse model that would allow us to better close the conceptual gap between the bench and the clinic. We also sought to affirm the advantages of metabolic cooperativity as directed towards relevant organs in the management of the disorder.

In this report, we describe a novel pure murine nonobese diabetic (NOD)/severe combined immunodeficiency (SCID)/Fabry line that supports human hematopoiesis. Furthermore, we demonstrate that the metabolic cooperativity effect led to reduced levels of Gb_3 in key organs over human HSC transplantation alone. This study provides crucial preclinical data for a Fabry gene therapy trial and validates this model for gauging the effectiveness of novel human cell-based therapies for Fabry disease.

Correspondence: *Jeffrey A Medin, Department of Medical Biophysics, UHN, Canadian Blood Services Building Room 406, 67 College Street, Toronto, Ontario, Canada M5G 2M1. E-mail: jmedin@uhnres.utoronto.ca*

RESULTS

Characterization of NOD/SCID/Fabry mice

Eleven backcrossings were performed starting from parental female-Fabry mice[17] and male-NOD/SCID mice. Throughout the breeding program, we performed an exhaustive analysis of the genotype (Fabry and NOD/SCID) and phenotype (deficient α-gal A enzyme activity in plasma; absence of T and B cells in peripheral blood (PB)) of the females in order to select the optimal breeders for the next generation and to ensure that genetic drift or "leakiness" of the mutations had not occurred (data not shown). Fabry-carrier homozygous NOD/SCID females were obtained at the third generation (F_3). As expected, the NOD/SCID genetic background content of the F_{11}-mice was >99% (data not shown), demonstrating that the new NOD/SCID/Fabry (NSF) line was fully congenic. The absence of T and B cells in the PB, as well as the lack of α-gal A activity in plasma confirmed the NSF phenotype of this novel line (**Figure 1a,b**). The α-gal A deficiency was also evident in the heart, kidney, spleen, liver, and lung (**Figure 1c**), which contributed to a significant accumulation of Gb_3 in the same organs (**Figure 1d**). Importantly, we found that all the biochemical parameters analyzed in this new model were comparable to results from the preexisting Fabry mouse (**Figure 1b–d**). Finally, F_{11}-mice were intercrossed and subsequently all the F_{13}-females and -males were homozygous or hemizygous for the Fabry genotype, respectively.

High levels of α-gal A activity *in vitro* achieved by lentiviral vector-mediated gene transfer into human hematopoietic cells

We have previously demonstrated that Gb_3 accumulation in tissues was completely prevented by neonatal injections of a recombinant lentiviral vector (LV) carrying the wild-type α-gal A cDNA as well as the selectable marker hCD25 cDNA (LV-α-gal A/internal ribosome entry site (IRES)/hCD25).[16] Here, using the same

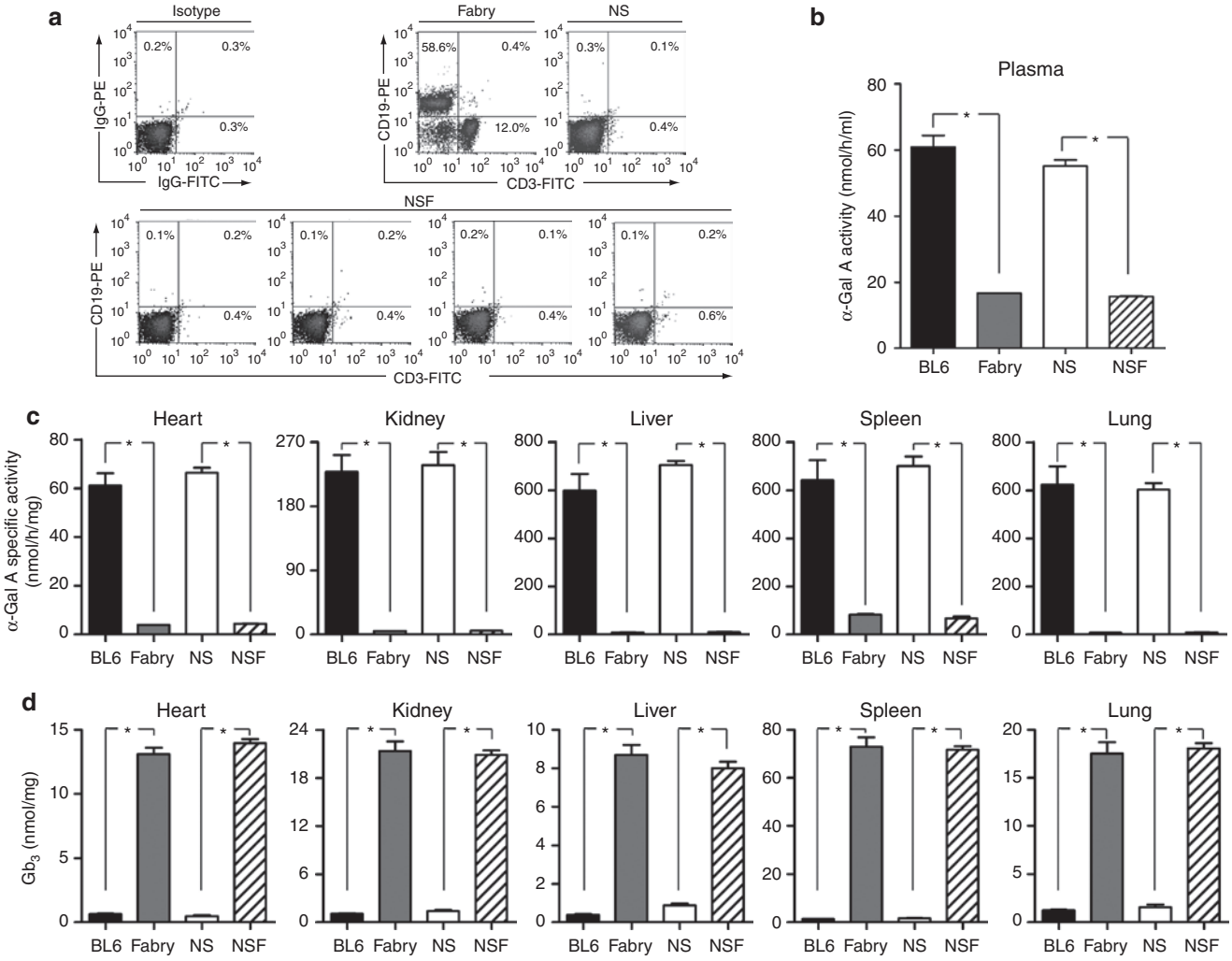

Figure 1 Phenotypic characterization of the novel NOD/SCID/Fabry xenograft model. Eleven generations of backcrossings were performed to generate a fully congenic NOD/SCID/Fabry line. At each generation different phenotypic studies were performed. (**a**) Representative flow cytometry analysis of the percentage of T and B cells in peripheral blood. Different F_{11}-individuals were compared with the parental mouse lines. (**b**) Plasma α-gal A enzyme activity was analyzed for the new mouse line and also compared to an earlier Fabry mouse model. (**c**) Specific enzyme activity in different organs. (**d**) Gb_3 quantification by HPLC. Data represent mean ± SD from five individuals (F_{11}) per group. *$P < 0.001$ compared to wild-type control groups. α-gal A, α-galactosidase A; BL6, wild-type; Fabry, traditional Fabry mice; FITC, fluorescein isothiocyanate; Gb_3, globotriaosylceramide; HPLC, high-performance liquid chromatography; NOD, nonobese diabetic; NSF, NOD/SCID/Fabry; NS, NOD/SCID; SCID, severe combined immunodeficiency.

vector (Figure 2) we transduced human cells including: K562 cells, Fabry patient B cells, and HSCs, and tested the therapeutic potential of this vector *in vitro*. We found that with a multiplicity of infection as low as 10, it was possible to modify ~70% and ~40% of the K562 cells (**Supplementary Figure S1a**) and Fabry patient B cells (**Supplementary Figure S1c**), respectively. Concomitantly, the intracellular α-gal A specific activity was increased more than tenfold and fourfold, respectively, in comparison to the LV-enhanced green fluorescent protein (eGFP) transduced control cells (**Supplementary Figure S1b,d**). As expected, this led to increased enzyme diffusion (ninefold and twofold for the K562 and Fabry B cells, respectively) (**Supplementary Figure S1b,d**). Next, we transduced normal human mobilized PB CD34$^+$ cells (Figure 3a) at a multiplicity of infection of 15 and evaluated outcomes *in vitro*. Four days after lentiviral infection, flow cytometry analyses revealed that on average, 51 ± 14% and 36 ± 10% (n = 3) of the human progenitor cells were positive for expression of the downstream selectable marker originating from our bicistronic LV construct or from LV-eGFP, respectively (Figure 3b). Similar results obtained 14 days after transduction demonstrate the stable nature of the transgenes (data not shown). Clonogenic studies (Figure 3c) showed no differences in the total number of colonies nor in the percentage of the different lineages among the groups (LV-α-gal A/IRES/hCD25 versus LV-eGFP or nontransduced control cells). PCR analysis[18] showed the expected proportion of vector-positive colonies (nontransduced cells: 0/90, LV-eGFP: 28/92, and LV-α-gal A/IRES/hCD25: 46/96). Moreover, by using the LV-α-gal A/IRES/hCD25 vector, the α-gal A activity of the enzymatically normal CD34$^+$ cells was increased more than twofold in comparison to the nontransduced or LV-eGFP transduced control cells (Figure 3d). Taken together, these data suggest that the gross physiology of the HSCs was not affected by the lentiviral infection or by transgene expression in this case.

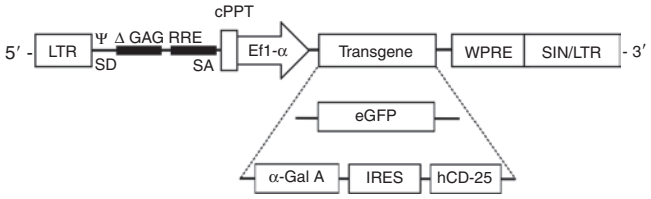

Figure 2 Lentivector schema. Schema of the lentivectors used in the present study. Control vector, LV-eGFP, and therapeutic vector, LV-α-gal A/IRES/hCD25. α-gal A, α-galactosidase A; cPPT, central polypurine tract; EF1-α, elongation factor 1-α promoter; eGFP, enhanced green fluorescent protein; IRES, internal ribosome entry site; LTR, long terminal repeat; RRE, Rev responsive element; SA, 3′ splice acceptor site; SD, 5′ splice donor site; SIN, self-inactivating LTR; WPRE, woodchuck hepatitis virus post-transcriptional regulatory element; ψ, human immunodeficiency virus packaging signal.

Human cell engraftment into NSF mice

Next, we performed two independent transplantations using normal human HSCs into separate NSF mice cohorts as described below. Cells were injected intravenously into 8-week-old male NSF mice (8×10^5 cells/mouse, 6–10 mice/group/experiment). Engraftment of the human hematopoietic cells was regularly evaluated (4, 6, 8, 10, and 12 weeks after transplantation) by determining the percentage of hCD45$^+$ cells in the PB of recipient mice (Figure 4a). As shown in Figure 4b, at 4 weeks after transplant, ~2% of the total white blood cells were derived from the injected human HSCs (for both experimental groups LV-eGFP and LV-α-gal A/IRES/hCD25).

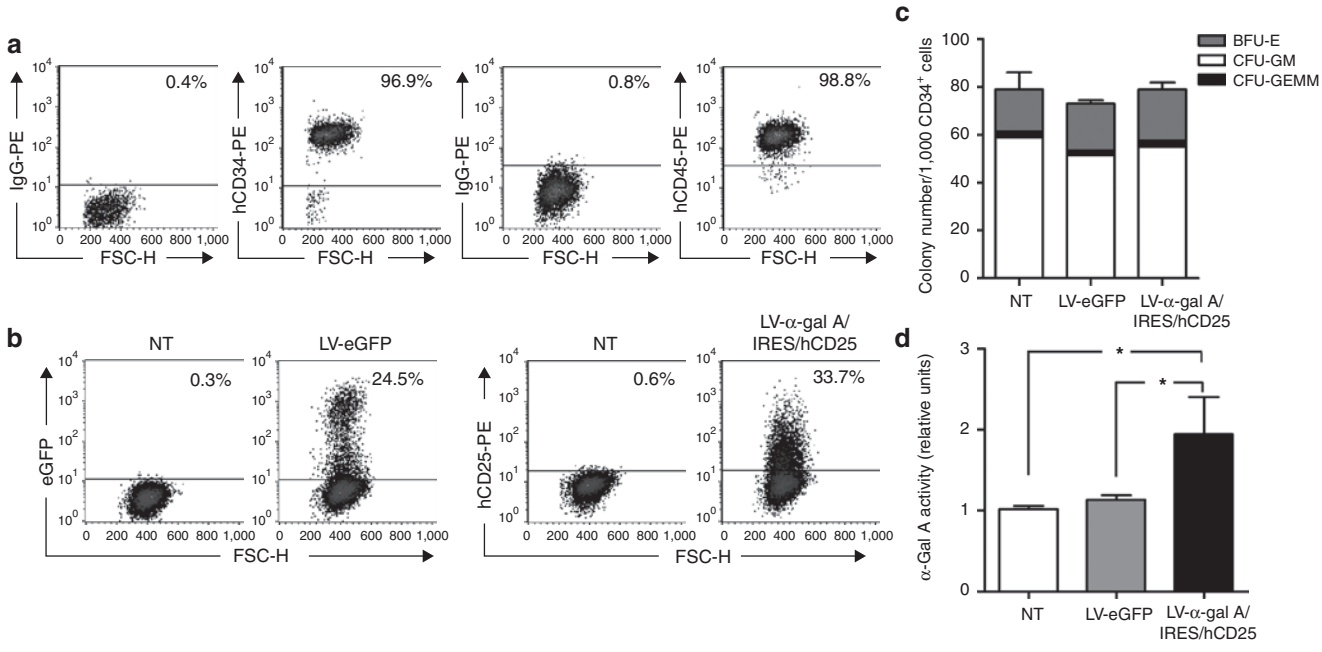

Figure 3 Phenotypic characterization of LV-transduced human CD34$^+$ progenitor cells. (**a**) Representative flow cytometry analysis of the normal human CD34$^+$ cells used in the *in vivo* experiment. (**b**) Percentage of eGFP or hCD25$^+$ cells at 4 days after transduction of the progenitor cells. A representative flow cytometry analysis is shown. (**c**) Representative clonogenic assay evaluated at 14 days after transduction. (**d**) Progenitor enzymatic activity evaluated 14 days after transduction. Data are mean ± SD (n = 3). *P < 0.01 compared to NT or LV-eGFP control cells. α-gal A, α-galactosidase A; BFU-E, burst-forming unit-erythroid; CFU-GM, colony-forming unit-granulocyte and macrophage; CFU-GEMM, colony-forming unit-granulocyte, erythrocyte, macrophage, and megakaryocyte; eGFP, enhanced green fluorescent protein; FSC-H, forward scatter; IRES, internal ribosome entry site; LV, lentiviral vector; NT, nontransduced cells.

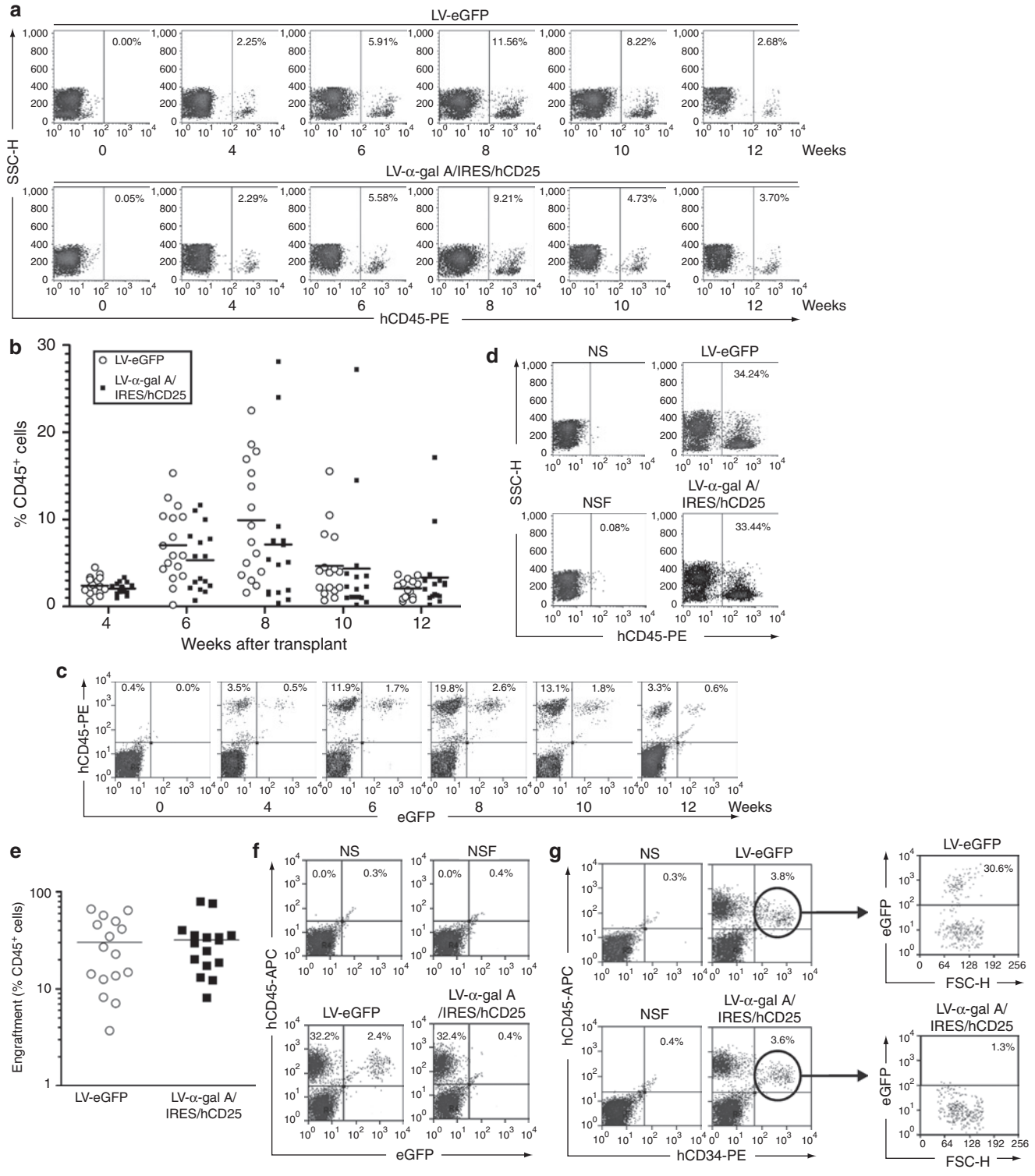

Figure 4 High level of engraftment of human HSCs in NOD/SCID/Fabry mice. Transduced progenitor cells (8×10^5) were injected intravenously into sublethally irradiated NOD/SCID/Fabry mice. (**a**) Representative flow cytometry analysis of the percentage of hCD45$^+$ cells in peripheral blood at different time points. (**b**) Percentage of hCD45$^+$ cells in peripheral blood analyzed by flow cytometry at different time points. (**c**) Representative flow cytometry analysis for LV-eGFP positive cells in circulation. (**d**) Representative dot-plot analysis of human cell engraftment from bone marrow samples 12 weeks after transplantation. (**e**) Bone marrow engraftment of human cells in all mice evaluated 12 weeks after transplant. (**f**) Representative hCD45$^+$/eGFP$^+$ cell engraftment analysis from pooled bone marrow samples. (**g**) Percentage of hCD34$^+$/eGFP$^+$ cells in bone marrow pools. Each open circle or black square represents an individual mouse. Two independent experiments were performed. α-gal A, α-galactosidase A; APC, allophycocyanin; eGFP, enhanced green fluorescent protein; FSC-H, forward scatter; HSC, hematopoietic stem cells; IRES, internal ribosome entry site; LV, lentiviral vector; NOD, nonobese diabetic; NSF, NOD/SCID/Fabry; NS, NOD/SCID; SCID, severe combined immunodeficiency; SSC-H, side scatter.

The percentage of hCD45$^+$ cells rapidly increased reaching a maximum at 8 weeks after infusions (**Figure 4b**) before declining again by the 10th week. It is worthwhile to mention that no differences in engraftment were observed between the groups at any of the evaluated times. Moreover, the presence of LV-eGFP positive cells in circulation demonstrated that this new model allows not only the engraftment of modified human cells but also their proliferation and differentiation (**Figure 4c**). Similar flow cytometry engraftment analyses were performed on bone marrow cells at euthanization (12 weeks after transplantation). As denoted in **Figure 4d,e**, a high percentage of hCD45$^+$ cells was observed in the bone marrow of the transplanted mice (30 ± 21% and 32 ± 20% for the LV-eGFP and LV-α-gal A/IRES/hCD25 groups, respectively) demonstrating no differences in the level of chimerism between both experimental groups. The feasibility of engraftment of the modified cells was confirmed by the presence of eGFP positive cells in the bone marrow (**Figure 4f**) of the transplanted mice. One interesting point is that ~30% of the hCD34$^+$ cells found in the bone marrow expressed the control transgene showing that multipotent human hematopoietic cells had been transduced (**Figure 4g**). Furthermore, no differences were observed in multilineage progenitor cell analyses performed on the bone marrow pools (hCD45$^+$ cells: ~31 ± 9%; hCD19$^+$ cells: ~25 ± 6%, and hCD33$^+$cells: ~6 ± 3%).

α-Gal A activity augmentation along with significant organ Gb_3 reductions in LV-α-gal A/IRES/hCD25 transplanted mice

To evaluate the outcome of the LV-mediated gene therapy approach in this novel xenograft model, we first analyzed the plasma α-gal A activity after transplantation. Even though no hCD25$^+$ cells were detectable in circulation (data not shown), the α-gal A activity in the plasma was significantly increased at all the evaluated time points (**Figure 5a**). Although the LV-eGFP group exhibited enzyme activity that was similar to pretransplantation levels, the LV-α-gal A/IRES/hCD25 experimental group showed an increase in plasma α-gal A activity of up to 20% (**Figure 5a**). As expected, a significant increase in the α-gal A enzyme activity was observed in the bone marrow cells, spleen, and liver of the LV-α-gal A/IRES/hCD25 group at 12 weeks after infusion (**Figure 5b**). At killing, organs were harvested from transplanted animals and the Gb_3 content was measured by detailed high-performance liquid chromatography analyses. As shown in **Figure 5c**, liver, lung, and spleen showed a significant decrease in Gb_3 content prompted by the infusion of normal cells (LV-eGFP versus nontransplanted NSF mice). In contrast, key organs in the pathophysiology of Fabry disease, specifically the heart and kidneys, did not benefit by the infusion of the control-transduced normal human CD34$^+$ cells (LV-eGFP group). Importantly however, Gb_3 content in these key organs, as well as liver, lung, and spleen, was significantly reduced in mice transplanted with the LV-α-gal A/IRES/hCD25-therapeutically modified cells (**Figure 5c**). This demonstrates that LV-mediated transduction has the capacity to mediate broader systemic correction through metabolic cooperativity.

In order to begin to explain the differences in Gb_3 reduction in tissues among both transplanted cohorts, in another experiment we infused 2.5 × 10^6 engineered-hCD34$^+$ cells (~20% LV-eGFP positive cells) into NSF mice and analyzed the tissue distribution of these modified human cells 8 weeks after transplant. As shown in **Figure 5d**, PB, bone marrow, and spleens of these mice harbored LV-eGFP–transduced cells that correlated well with the augmentation of α-gal A enzyme observed in such tissues (**Figure 5a,b**). Similar results were obtained by immunostaining for the eGFP protein; while heart and kidney were negative (data not shown). These data suggest that there is localized enzyme production in the organs and that the bone marrow and spleen are major contributors that secrete enzyme into the circulation, elevating systemic α-gal A levels. Interestingly, rare eGFP positive cells were found in the brain of the transplanted mice (data not shown) suggesting that a gene therapy approach may have advantages over ERT, for example, for correcting the cerebrovascular manifestations of Fabry disease. Lastly, it is worth noting that in this experiment the genetic modification of long-term progenitor cells did not affect their normal differentiation into hCD3$^+$, hCD19$^+$, hCD33$^+$, and hCD14$^+$ cells, and that the transgene was equally expressed in all the lineages (**Figure 5d**).

DISCUSSION

In this study, we have generated a novel NSF mouse model that accepts xenogeneic HSC transplantation. Moreover, by using this model we demonstrated that genetically modified bone marrow cell transplantation improves outcomes, as measured by Gb_3 accumulation, over HSC transplantation alone. While the generation of a Fabry mouse[17] represented a milestone for the field, we sought a more directly translational model that allows us to work with human cells and evaluate the consequences of therapeutic intervention. This novel model also facilitates our collection of key preclinical data for future implementation of a gene therapy trial for Fabry disease as toxicity and efficiency measurements can be made on the true target population in an *in vivo* setting.

We generated this fully congenic xenograft model by changing the genetic background of the pre-existent Fabry mouse through eleven generations of backcrossings. Our NSF mice exhibited a deficiency of α-gal A activity and progressive Gb_3 accumulation, but also did not mimic the clinical symptoms of Fabry disease. Studies performed in a previous Fabry mouse model revealed that the murine erythrocytes, a likely source of Gb_3 in humans, do not contain appreciable level of Gb_4 (Gb_3 precursor) or even Gb_3 itself suggesting that the lipid accumulation in mice would be milder than in humans.[19] However, considering that by thin layer chromatography lipid analysis we were able to observe small amounts of Gb_4 as well as Gb_3 accumulation in packed NSF erythrocytes (data not shown), this earlier explanation may not be directly translatable to our current model. In this regard, more studies have to be performed in order to elucidate the mechanisms that make this murine model less susceptible to typical Fabry disease manifestations.

Some clinical studies have recognized that the best outcomes may be achieved by increasing the frequency of administration of α-gal A, suggesting that cells/tissues may require a continuous presence of the enzyme.[20,21] It has been previously postulated that only 15–20% of the normal α-gal A activity is sufficient to mediate significant clinical improvements.[22] We have shown that this level of efficiency is feasible and that a long-term, and continuous production of enzyme can be achieved through the lentiviral infection of bone marrow cells followed by transplantation.[23] In our

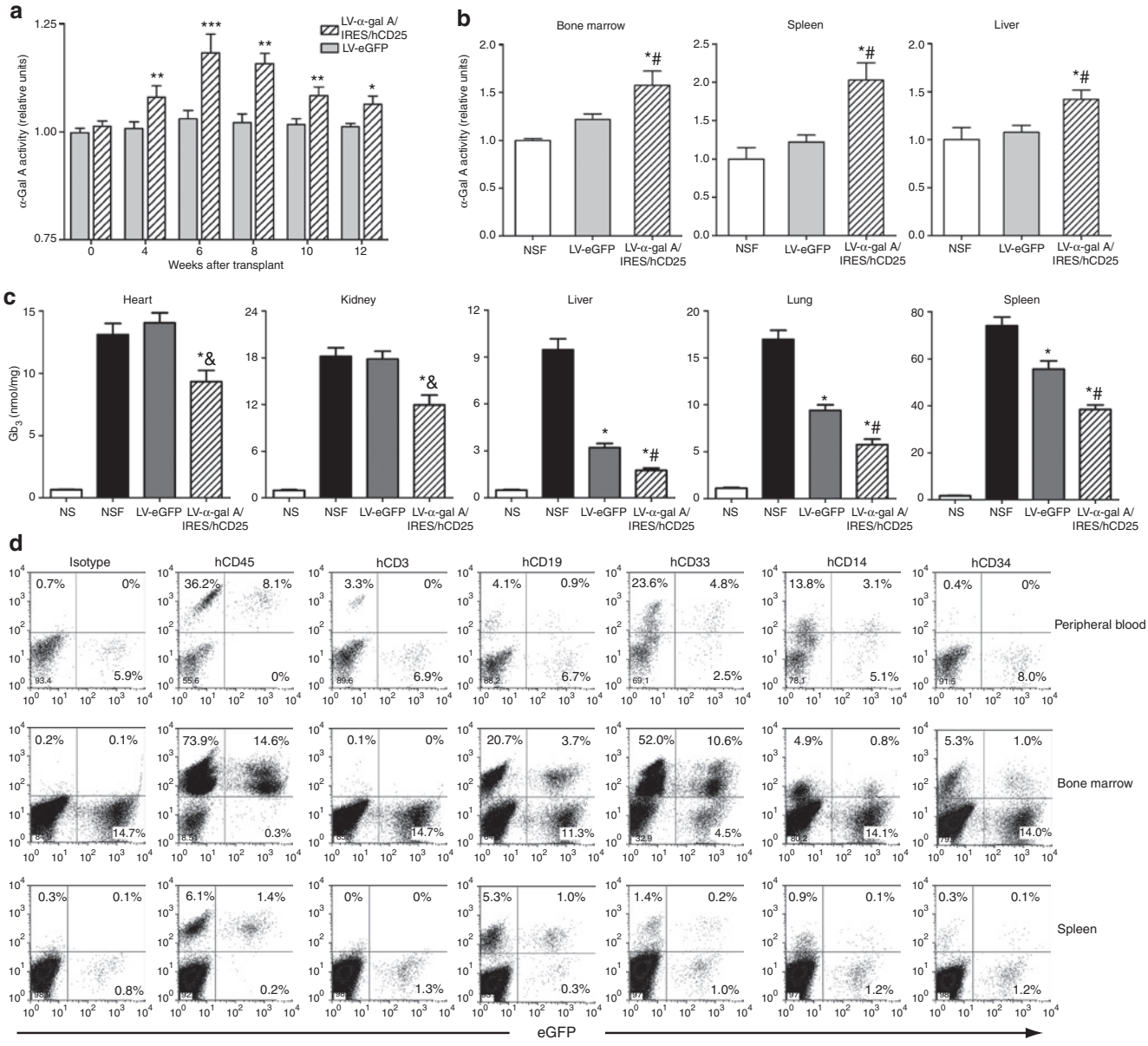

Figure 5 α-Gal A activity augmentation and organ Gb_3 reduction in the LV-α-gal A/IRES/hCD25 transplanted mice. (**a**) Plasma α-gal A enzyme activity was evaluated at 4, 6, 8, 10, and 12 weeks after transplantation. Data were normalized to nontransplanted NOD/SCID/Fabry mice enzyme levels and represent mean ± SEM ($n = 16$). *$P < 0.05$, **$P < 0.01$, and ***$P < 0.001$ compared to the LV-eGFP control group. (**b**) Bone marrow, spleen, and liver α-gal A enzyme activity at killing. Data represent mean ± SEM ($n = 16$). *$P < 0.01$ compared to nontransplanted group and $^{\#}P < 0.05$ versus eGFP group. (**c**) HPLC-based Gb_3 quantification in heart, kidney, liver, lung, and spleen at 12 weeks after transplantation. Data represent mean ± SEM ($n = 16$). *$P < 0.01$ compared to nontransplanted group and $^{\&}P < 0.01$ or $^{\#}P < 0.05$ versus the LV-eGFP group. (**d**) Representative flow cytometry analyses of engineered cell tissue engraftment. α-gal A, α-galactosidase A; eGFP, enhanced green fluorescent protein; Gb_3, globotriaosylceramide; IRES, internal ribosome entry site; LV, lentiviral vector; NOD, nonobese diabetic; NSF, NOD/SCID/Fabry; NS, NOD/SCID; SCID, severe combined immunodeficiency.

experiments, we did not observe significant Gb_3 reduction in the heart and kidneys of the control transplanted mice. Consequently, we propose that allogeneic bone marrow transplantation, as represented by the LV-eGFP control group, may be insufficient to mediate treatment in these organs, meaning that the amount of enzyme that was secreted by normal cells was not enough to reach therapeutic levels in circulation. Moreover, the significant lipid reduction observed in liver, lung, and spleen of the eGFP mice group may be, in essence, a localized effect. It has been described that in NOD/SCID transplanted mice most of the human progenitor cells usually engraft in the bone marrow, spleen, and liver.[24–26] Our data are consistent with those findings as we showed a significant increase in the α-gal A activity in those same organs. We also showed increases in α-gal A activity in the plasma of the therapeutically transplanted group, reaffirming not only the improved therapeutic outcomes of the LV-α-gal A/IRES/hCD25 transduced cohort in such localized tissues, but that potent cross-correction effects likely mediate correction of the hearts and kidneys of the experimental group.

LV-modified autologous cells offer several advantages in comparison to allogeneic bone marrow transplantation for treatment

of lysosomal storage disorders. First, the use of autologous cells would reduce the morbidity and mortality associated with the procedure. Second, the risks of graft-versus-host disease would be abolished. Lastly, as we have shown here, engineered cells can express much higher levels of the therapeutic enzyme, rendering them more effective than transplanted wild-type cells. In spite of being unable to detect the expression of the hCD25 selectable marker at appreciable levels (less than 1%, data not shown) in the PB, the increase in the α-gal A activity was clearly noted in the plasma, spleen, liver, and bone marrow cell samples. This lower marker expression could be related to the activation of different clones in the bone marrow resulting in an *in vivo* $hCD25^+$ cell dilution or a lower expression of the second transgene compared to the first one (the α-gal A gene in this case). Indeed, it has been previously demonstrated that in a bicistronic construct with an IRES element, the efficiency of expression of the second gene is usually lower than the first one, with the expression level varying from 6 to 100% (relative to first gene expression), depending on cell types and reporter genes.[27] Enzyme-secreting cells could have also engrafted in regions not sampled by PB analyses.

In summary, these results show that our novel NSF mouse model exhibits a deficiency in α-gal A activity with typical Gb_3 accumulation as observed in Fabry disease, but also can accept transplanted human $CD34^+$ cells. Gb_3 accumulation in this novel xenograft model was partially corrected by infusion of normal human $CD34^+$ cells. However, the greatest benefits were mediated by infusion of genetically modified $CD34^+$ cells. These results support the idea that allogeneic bone marrow transplantation by itself is not sufficient to achieve adequate levels of metabolic cooperativity and suggest gene therapy as a focus for correction of Fabry disease and other lysosomal storage disorders.

MATERIAL AND METHODS

Development of the NSF mouse. α-Gal A-deficient Fabry mice[17] were bred at the Animal Resource Center, University Health Network (UHN). NOD.CB17-*Prkdc*^{scid} (NOD/SCID) mice were purchased from Jackson Laboratories (Bar Harbor, ME) and bred in a colony maintained at UHN. Animal experimentation protocols were approved by the UHN Animal Care Committee. The parental generation (F_0) consisted of Fabry female (α-gal $A^{-/-}scid^{+/+}$) and NOD/SCID male (α-gal $A^{+/0}scid^{-/-}$) mice. F_1-double heterozygous female mice (α-gal $A^{+/-}scid^{+/-}$) were mated with NOD/SCID male mice to generate α-gal $A^{+/-}scid^{-/-}$ female mice (F_2). For all the backcrosses, the NSF-offspring genotype was analyzed from tail DNA following Jackson Laboratories and Ohshima *et al.*[19] conditions, respectively. Nine additional generations (F_3–F_{11}) were prepared by backcrossing heterozygous Fabry females (α-gal $A^{+/-}scid^{-/-}$) with NOD/SCID males. The F_{11}-genetic background was determined by NOD/SCID genomic scanning (225 single-nucleotide polymorphisms were analyzed) at the Jackson Laboratories. Mice harboring >99% NOD/SCID genetic background were selected and interbred to obtain the double homozygous female mice (F_{12}). The pure NSF line (F_{13}) was finally achieved by breeding the homozygous Fabry female mice (F_{12}) with the hemizygous male mice (F_{12}). The NSF phenotype was also confirmed by determining the absence of mature T and B cells by flow cytometry, assessment of the specific α-gal A enzyme activity, and evaluation of organ Gb_3 accumulation by high-performance liquid chromatography (see below). Fabry mice[17] and NOD/SCID mice (as above) were also used as controls.

α-Gal A activity assay and Gb3 quantification. The specific α-gal A activity was determined by fluorometric assay as previously described.[16] Briefly, plasma or cells/organs protein extracts were incubated with 4-methylumbelliferyl-α-D-galactopyranoside (5 mmol/l) (RPI, Mount Prospect, IL) in presence of the α-N-acetylgalactosaminidase inhibitor, N-acetyl-D-galactosamine (100 mmol/l) (Sigma, Oakville, Ontario, Canada). The product of the enzymatic reaction was quantified by comparison with known concentrations of 4-methylumbelliferone. Mouse organ Gb_3 content was determined by high-performance liquid chromatography as described.[19] Each measurement was assessed in triplicate, and normalized to total protein concentration (DC^T Protein Assay; Bio-Rad Laboratories, Mississauga, Ontario, Canada).

Vectors and lentivirus production. The LV pHR′cPPT-EF1α-α-gal A-IRES-hCD25-WPRE-SIN (LV-α-gal A/IRES/hCD25) was previously constructed in our lab.[16] Vesicular stomatitis virus glycoprotein-pseudoptyped lentiviruses (VSVg-LVs), including an eGFP control vector (LV-eGFP), were generated as described[23] by cotransfection of the LV plasmid construct (LV-eGFP or LV-α-gal A/IRES/hCD25) in combination with the packaging (pCMVΔR8.91) and VSVg envelope-coding (pMD.G) plasmids into HEK 293T cells. Viral supernatants were harvested 48 hours later and concentrated by ultracentrifugation at 50,000*g* for 2 hours. Viral stocks were resuspended in phosphate-buffered saline containing bovine serum albumin (1% wt/vol) and stored at −80 °C until use. LV suspensions were serially diluted and functionally titered on HEK 293T cells by analyzing the transgene expression by flow cytometry. Titers of each of the LV preparations were higher than 1×10^9 functional infectious particles/ml as measured by eGFP and hCD25 expression analyses (data not shown).

Cell transduction and transplantation protocol. K562 (human erythroleukemic cells) cells and Fabry patient B cells[12] were cultured in RPMI-1640 media (Sigma) supplemented with 10% fetal bovine serum (PAA, Toronto, Ontario, Canada), 2 mmol/l glutamine, 100 U/ml penicillin, and 100 mg/ml streptomycin (all from Invitrogen, Carlsbad, CA) and maintained in a humidified incubator at 37 °C in an atmosphere containing 5% CO_2. Human mobilized PB $CD34^+$ cells were obtained from AllCells (Emeryville, CA). These cells were rapidly thawed following the manufacturer's recommendations. After thawing, ~85% of the cells were viable as assessed by trypan blue exclusion, while the hCD34 expression was higher than 90% as determined by flow cytometry analysis. Cells were prestimulated for 24 h in StemSpan media (Stemcell Technologies, Vancouver, British Columbia, Canada) supplemented with SCF (100 ng/ml), Flt-3 (50 ng/ml), TPO (50 ng/ml), and IL-6 (20 ng/ml) (all from R&D System, Minneapolis, MN). Cells were then resuspended in concentrated LV supernatants (LV-eGFP or LV-α-gal A/IRES/hCD25) at a concentration of 1×10^6 cells/ml and cultured overnight on Fibronectin (5 μg/cm^2; Sigma) coated plates. Vector supernatants were added at a functional multiplicity of infection of 15 and supplemented with the aforementioned cytokine cocktail plus 8 mg/ml protamine sulfate (Sigma). Flow cytometry analysis was performed 72 hours later to examine eGFP or hCD25 expression on mobilized PB $CD34^+$ cells. Clonogenic assays were also performed following manufacturer's recommendations (Stemcell Technologies) while the assessment of vector-positive cells was analyzed as described.[18]

Recipient mice were sublethally irradiated (300cGy) and injected intraperitoneally with 200 μg of purified anti-CD122 antibody 24 hours before transplantation for natural killer cell depletion as described.[28] Vector transduced cells (8×10^5/mouse) were injected into the tail vein of 8-week-old NSF male mice. Age- and sex-matched NSF and NOD/SCID mice were used as untouched or wild-type controls, respectively. Mice were analyzed up to 12 weeks after transplantation.

Flow cytometry analysis. Single-cell suspensions of PB and bone marrow were generated following collection from mice at the time of analysis. Red blood cells were lysed in ammonium chloride (150 mmol/l), potassium bicarbonate (10 mmol/l), and ethylenediaminetetraacetic acid (0.1 mmol/l) for 5 minutes at 37 °C (all from Sigma). Cells were washed with phosphate-buffered saline and resuspended in FACS buffer (phosphate-buffered

saline, 0.5% fetal bovine serum, and 2 mmol/l ethylenediaminetetraacetic acid) on ice and stained with the appropriate antibody. The following antibodies were used: hCD25-PE, hCD45-APC, hCD45-PE, hCD34-PE, hCD19-PE, hCD33-PE, hCD14. All antibodies were obtained from BD Biosciences (Mississauga, Ontario, Canada). Cells were then analyzed by flow cytometry using a FACSCalibur (BD) and data were analyzed using CellQuestPro software (BD).

Statistical analysis. Results are expressed as mean ± SD or SEM as indicated and are representative of two independent experiments with 6–10 animals per group. Differences between groups were assessed using Student's *t*-test or analysis of variance. Values of $P < 0.05$ were considered to be statistically significant.

SUPPLEMENTARY MATERIAL

Figure S1. High intracellular levels of α-gal A activity and secretion *in vitro* mediated by therapeutic LV transduction.

ACKNOWLEDGMENTS

We thank members of the Medin Lab for help with bone marrow collections and organ harvests. We thank Mark Sands for discussions. This research was funded by a research operating grant from the Canadian Institutes of Health Research to J.A.M. The authors declared no conflict of interest.

REFERENCES

1. Brady, RO, Gal, AE, Bradley, RM, Martensson, E, Warshaw, AL and Laster, L (1967). Enzymatic defect in Fabry disease: ceramidetrihexosidase deficiency. *N Engl J Med* **276**: 1163–1167.
2. MacDermot, KD, Holmes, A and Miners, AH (2001). Anderson-Fabry disease: clinical manifestations and impact of disease in a cohort of 98 hemizygous males. *J Med Genet* **38**: 750–760.
3. MacDermot, KD, Holmes, A and Miners, AH (2001). Anderson-Fabry disease: clinical manifestations and impact of disease in a cohort of 60 obligate carrier females. *J Med Genet* **38**: 769–775.
4. Schiffmann, R (2006). Neuropathy and Fabry disease: pathogenesis and enzyme replacement therapy. *Acta Neurol Belg* **106**: 61–65.
5. Lidove, O, Joly, D, Barbey, F, Bekri, S, Alexandra, JF, Peigne, V *et al.* (2007). Clinical results of enzyme replacement therapy in Fabry disease: a comprehensive review of literature. *Int J Clin Pract* **61**: 293–302.
6. Rohrbach, M and Clarke, JT (2007). Treatment of lysosomal storage disorders: progress with enzyme replacement therapy. *Drugs* **67**: 2697–2716.
7. Moore, DF, Ries, M, Forget, EL and Schiffmann, R (2007). Enzyme replacement therapy in orphan and ultra-orphan diseases: the limitations of standard economic metrics as exemplified by Fabry-Anderson disease. *Pharmacoeconomics* **25**: 201–208.
8. Breunig, F, Weidemann, F, Strotmann, J, Knoll, A and Wanner, C (2006). Clinical benefit of enzyme replacement therapy in Fabry disease. *Kidney Int* **69**: 1216–1221.
9. Schiffmann, R, Askari, H, Timmons, M, Robinson, C, Benko, W, Brady, RO *et al.* (2007). Weekly enzyme replacement therapy may slow decline of renal function in patients with Fabry disease who are on long-term biweekly dosing. *J Am Soc Nephrol* **18**: 1576–1583.
10. Thofehrn, S, Netto, C, Cecchin, C, Burin, M, Matte, U, Brustolin, S *et al.* (2009). Kidney function and 24-hour proteinuria in patients with Fabry disease during 36 months of agalsidase alfa enzyme replacement therapy: a Brazilian experience. *Ren Fail* **31**: 773–778.
11. Caballero, L, Climent, V, Hernández-Romero, D, Quintanilla, MA, de la Morena, G and Marín, F (2010). Enzyme replacement therapy in Fabry disease: influence on cardiac manifestations. *Curr Med Chem* **17**: 1679–1689.
12. Medin, JA, Tudor, M, Simovitch, R, Quirk, JM, Jacobson, S, Murray, GJ *et al.* (1996). Correction in trans for Fabry disease: expression, secretion and uptake of alpha-galactosidase A in patient-derived cells driven by a high-titer recombinant retroviral vector. *Proc Natl Acad Sci USA* **93**: 7917–7922.
13. Takenaka, T, Hendrickson, CS, Tworek, DM, Tudor, M, Schiffmann, R, Brady, RO *et al.* (1999). Enzymatic and functional correction along with long-term enzyme secretion from transduced bone marrow hematopoietic stem/progenitor and stromal cells derived from patients with Fabry disease. *Exp Hematol* **27**: 1149–1159.
14. Takenaka, T, Murray, GJ, Qin, G, Quirk, JM, Ohshima, T, Qasba, P *et al.* (2000). Long-term enzyme correction and lipid reduction in multiple organs of primary and secondary transplanted Fabry mice receiving transduced bone marrow cells. *Proc Natl Acad Sci USA* **97**: 7515–7520.
15. Qin, G, Takenaka, T, Telsch, K, Kelley, L, Howard, T, Levade, T *et al.* (2001). Preselective gene therapy for Fabry disease. *Proc Natl Acad Sci USA* **98**: 3428–3433.
16. Yoshimitsu, M, Sato, T, Tao, K, Walia, JS, Rasaiah, VI, Sleep, GT *et al.* (2004). Bioluminescent imaging of a marking transgene and correction of Fabry mice by neonatal injection of recombinant lentiviral vectors. *Proc Natl Acad Sci USA* **101**: 16909–16914.
17. Ohshima, T, Murray, GJ, Swaim, WD, Longenecker, G, Quirk, JM, Cardarelli, CO *et al.* (1997). α-Galactosidase A deficient mice: A model of Fabry disease. *Proc Natl Acad Sci USA* **94**: 2540–2544.
18. Ramsubir, S, Nonaka, T, Girbés, CB, Carpentier, S, Levade, T and Medin, JA (2008). *In vivo* delivery of human acid ceramidase via cord blood transplantation and direct injection of lentivirus as novel treatment approaches for Farber disease. *Mol Genet Metab* **95**: 133–141.
19. Ohshima, T, Schiffmann, R, Murray, GJ, Kopp, J, Quirk, JM, Stahl, S *et al.* (1999). Aging accentuates and bone marrow transplantation ameliorates metabolic defects in Fabry disease mice. *Proc Natl Acad Sci USA* **96**: 6423–6427.
20. Schiffmann, R, Askari, H, Timmons, M, Robinson, C, Benko, W, Brady, RO *et al.* (2007). Weekly enzyme replacement therapy may slow decline of renal function in patients with Fabry disease who are on long-term biweekly dosing. *J Am Soc Nephrol* **18**: 1576–1583.
21. Schiffmann, R (2009). Fabry disease. *Pharmacol Ther* **122**: 65–77.
22. Beck, M (2010). *Fabry Disease.* Springer: Dordrecht, Heidelberg, London, New York. ch. 24, pp. 381–388.
23. Yoshimitsu, M, Higuchi, K, Ramsubir, S, Nonaka, T, Rasaiah, VI, Siatskas, C *et al.* (2007). Efficient correction of Fabry mice and patient cells mediated by lentiviral transduction of hematopoietic stem/progenitor cells. *Gene Ther* **14**: 256–265.
24. Noort, WA, Willemze, R and Falkenburg, JH (1998). Comparison of repopulating ability of hematopoietic progenitor cells isolated from human umbilical cord blood or bone marrow cells in NOD/SCID mice. *Bone Marrow Transplant* **22** (suppl. 1): S58–S60.
25. Hofling, AA, Vogler, C, Creer, MH and Sands, MS (2003). Engraftment of human CD34+ cells leads to widespread distribution of donor-derived cells and correction of tissue pathology in a novel murine xenotransplantation model of lysosomal storage disease. *Blood* **101**: 2054–2063.
26. Wulf-Goldenberg, A, Eckert, K and Fichtner, I (2008). Cytokine-pretreatment of CD34(+) cord blood stem cells *in vitro* reduces long-term cell engraftment in NOD/SCID mice. *Eur J Cell Biol* **87**: 69–80.
27. Mizuguchi, H, Xu, Z, Ishii-Watabe, A, Uchida, E and Hayakaw, T (2000). IRES-dependent second gene expression is significantly lower than cap-dependent first gene expression in a bicistronic vector. *Mol Ther* **1**: 376–382.
28. McKenzie, JL, Gan, OI, Doedens, M and Dick, JE (2005). Human short-term repopulating stem cells are efficiently detected following intrafemoral transplantation into NOD/SCID recipients depleted of CD122+ cells. *Blood* **106**: 1259–1261.